On the Impact of Lossy Compression on Hyperspectral Image Classification and Unmixing

Fernando García-Vílchez, Jordi Muñoz-Marí, Maciel Zortea, Ian Blanes, *Student Member, IEEE*,
Vicente González-Ruiz, Gustavo Camps-Valls, *Senior Member, IEEE*,
Antonio Plaza, *Senior Member, IEEE*, and Joan Serra-Sagristà, *Member, IEEE*

***Abstract*—Hyperspectral data lossy compression has not yet achieved global acceptance in the remote sensing community, mainly because it is generally perceived that using compressed images may affect the results of posterior processing stages. This possible negative effect, however, has not been accurately characterized so far. In this letter, we quantify the impact of lossy compression on two standard approaches for hyperspectral data exploitation: spectral unmixing, and supervised classification using support vector machines. Our experimental assessment reveals that different stages of the linear spectral unmixing chain exhibit different sensitivities to lossy data compression. We have also observed that, for certain compression techniques, a higher compression ratio may lead to more accurate classification results. Even though these results may seem counterintuitive, this work explains these observations in light of the spatial regularization and/or whitening that most compression techniques perform and further provides recommendations on best practices when applying lossy compression prior to hyperspectral data classification and/or unmixing.**

***Index Terms*—Endmember extraction, hyperspectral data lossy compression, image classification, linear spectral unmixing, principal component analysis (PCA), regularization, support vector machine (SVM), transform coding, wavelet transform.**

I. Introduction

In RECENT years, enormous data volumes have been collected by hyperspectral instruments such as NASA's Airborne Visible Infra-Red Imaging Spectrometer (AVIRIS) [1], which is able to cover the wavelength region from 0.4 to 2.5 μm using more than 200 spectral channels, at a nominal spectral resolution of 10 nm. In hyperspectral imaging, two types of compression have been investigated extensively in the past [2]. Lossless data compression is generally considered as data compaction, which eliminates *unnecessary* redundancy but without loss of information. In contrast, lossy data compression removes some *low-detail* information. Since the best compression ratios achieved by lossless techniques are in the order of 3:1 [3], lossy compression is used when higher ratios are required.

Nevertheless, lossy compression has not yet achieved global acceptance in the remote sensing community, because it is generally perceived that using compressed images may ultimately affect the results of posterior processing stages of remote sensing images, such as spectral unmixing or image classification. This negative effect, however, has been scarcely characterized, mostly in the context of classification applications [2]. In [4], an interesting observation was drawn: classification performance was not tightly related to distortion curves, i.e., the best classifiers based on rate-distortion curves did not generally offer the best classification accuracies. In addition, in [5], a vector quantization (VQ) approach was proposed for the joint classification and compression of hyperspectral images. In this case, compression ratios of 70:1 were achieved without reducing the classification performance noticeably. The authors proposed the classification error as an alternative to the mean-square-error (MSE) distortion measure. Similar achievements were reported in [6]–[8], where high classification accuracy was obtained at high compression ratios, particularly when a spatial–spectral (waveletlike) transform was applied. This suggests that including spatial information typically improves classification accuracy, even if this information is introduced through image distortion induced by lossy compression. An alternative approach would consider the joint compression and classification of the image through VQ-based approaches [5], [9], [10], yet this is out of the scope of this letter, in which we investigate the impact of lossy compression techniques on the different steps that comprise the linear spectral unmixing chain [11] and also on the various stages involved in nonlinear hyperspectral image classification using support vector machines (SVMs) [12]. In these two contexts, several questions need to be answered.

1) Does lossy compression substantially reduce accuracy in general-purpose image classification and spectral unmixing? This question is particularly important since, even though it is widely acknowledged that lossy compression decreases the quality of the image, there are also evidences stating that some kind of transform coding may be useful as a preprocessing step prior to classification.
2) How does the quality of information extraction correlate with the compression ratio in image classification and

Manuscript received October 17, 2009; revised March 7, 2010 and June 16, 2010; accepted July 15, 2010. Date of publication September 13, 2010; date of current version February 25, 2011. This work was supported in part by Project MRTN-CT-2006-035927, Project AYA2008-05965-C04-02/03, Project TEC2006-13845, Project CONSOLIDER CSD2007-00018, Project TIN2009-14426-C02-01, Project TIN2009-05737-E/TIN, Project TIN2008-01117, Project P08-TIC-3518, and Project FPU2008.

F. García-Vílchez, I. Blanes, and J. Serra-Sagristà are with the Department of Information and Communications Engineering, Escola d'Enginyeria, Universitat Autònoma de Barcelona, 08193 Bellaterra, Spain.

J. Muñoz-Marí and G. Camps-Valls are with the Image Processing Laboratory (IPL) and the Department Enginyeria Electrònica, Escola Tècnica Superior d'Enginyeria, Universitat de València, 46100 Burjassot, Spain.

M. Zortea and A. Plaza are with the Department of Technology of Computers and Communications. University of Extremadura, 10071 Cáceres, Spain.

V. González-Ruiz is with the Department of Computer Architecture and Electronics, University of Almería, 04120 Almería, Spain.

Color versions of one or more of the figures in this paper are available online at http://ieeexplore.ieee.org.

Digital Object Identifier 10.1109/LGRS.2010.2062484

TABLE I
FEATURE COMPARISON BETWEEN THE CCSDS-IDC RECOMMENDATION, TER, AND JPEG2000 COMPRESSION TECHNIQUES, INCLUDING QUALITY (L), POSITION (P), RESOLUTION (R), AND COMPONENT (C) SCALABILITY

	CCSDS-IDC [13]	TER [14]	JPEG2000 [15]
Spatial DWT levels	3	any	any
Multiband compression	no	yes	yes
Spectral transform	none	none/DWT/PCA	none/DWT/PCA
Stream scalability	L	L, P, R, and C	L, P, R, and C
Interactive decoding	no	yes	yes
Interactive transmission	no	yes	yes
Complexity	low	low	high

spectral unmixing? Answering this question would allow us to assess the relative importance of the compression stage, e.g., in some application domains, working with largely compressed images may not constitute a problem even at the cost of reduced accuracies.

3) What are the steps in the classification and spectral unmixing processing chains that are affected the most? Answering this question is crucial to fully characterize the sensitivity of the different steps involved in the information extraction processes (in our case, classification and spectral unmixing) to lossy compression.

The remainder of this letter is organized as follows: Section II describes the lossy compression techniques used in our experiments. Section III substantiates the impact of lossy compression on the different stages of linear spectral unmixing and SVM-based classification. Section IV draws some conclusions.

II. LOSSY COMPRESSION TECHNIQUES

All the progressive lossy-to-lossless compression techniques considered in this work are wavelet based. Wavelet-based compression techniques are commonly divided into two functional parts: First, a discrete wavelet transform (DWT) decorrelates the input image in the spatial domain, and second, a bit plane encoder (BPE) stage encodes the transformed image, possibly followed by an entropy coder (e.g., a Huffman or an arithmetic encoder). In addition, in order to improve the coding performance of these techniques, a common strategy for hyperspectral images is to decorrelate first the image in the spectral domain; DWT and principal component analysis (PCA) are often used as spectral decorrelator [4].

The compression techniques selected for our evaluation are the Recommendation for Image Data Compression (IDC) [13] designed by the Consultative Committee for Space Data Systems (CCSDS) (we refer to this technique as to CCSDS-IDC for short); TER [14], an extension of the CCSDS-IDC Recommendation for remote sensing scenarios; and the latest standard of the Joint Photographic Experts Group (JPEG) JPEG2000 [15]. The main similarities and differences between the CCSDS-IDC Recommendation, TER, and JPEG2000 are summarized in Table I.

Table II reports the progressive lossy-to-lossless techniques investigated in our research. For all the techniques, but for CCSDS-IDC, which is restricted to three, five levels of DWT have been applied in the spatial domain. When employed, five levels of DWT have also been applied in the spectral domain. CCSDS-IDC and JPEG-BIFR (JPEG2000 with Band Independent Fixed Rate) fix the same target bit rate for all components before the encoding process begins, whereas the rest of the techniques are able to distribute the target bit rate among the components using a bit allocation algorithm.

TABLE II
PROGRESSIVE LOSSY-TO-LOSSLESS TECHNIQUES

Compression technique	Spectral decorrelation	Target bit-rate	RD optimization	Software used
CCSDS-IDC	none	band fixed	none	TER [16]
JPEG2000-BIFR	none	band fixed	none	Kakadu [17]
TER	none	full volume	CPI [18]	TER
JPEG2000	none	full volume	PCRD [15]	Kakadu
DWT-TER	DWT	full volume	CPI	TER
DWT-JPEG2000	DWT	full volume	PCRD	Kakadu
PCA-TER	PCA	full volume	CPI	TER
PCA-JPEG2000	PCA	full volume	PCRD	BOI [19]

III. EXPERIMENTAL RESULTS

We investigate here the performance of the different progressive lossy-to-lossless techniques in terms of two hyperspectral data exploitation applications, i.e., linear spectral unmixing and pixel-based SVM classification. In all cases, the evaluation has been performed on a representative bit-rate range 0.2–2.0 bits per pixel per band (bpppb), i.e., a compression ratio ranging from 80:1 to 8:1, with a bit-rate step of 0.2 bpppb.

A. Linear Spectral Unmixing

The hyperspectral scene used for the linear spectral unmixing experiments is the well-known AVIRIS Cuprite reflectance data set.[1] This scene has been widely used to validate the performance of endmember extraction algorithms. The portion used in experiments corresponds to a 350×350 pixel subset of the sector labeled as f970619t01p02_r02_sc03.a.rfl in the online data. The scene comprises 224 spectral bands between 0.4 and 2.5 μm, with a nominal spectral resolution of 10 nm. Prior to the analysis, several bands were removed due to water absorption and low signal-to-noise ratio in those bands, retaining a total of 188 bands for experiments. The Cuprite site is well understood mineralogically and has several exposed minerals of interest, as reported by the U.S. Geological Survey (USGS) in the form of various mineral spectral libraries[2] used to assess endmember signature purity.

1) Experiment 1: Impact of Hyperspectral Data Lossy Compression on the Estimation of the Number of Endmembers: Fig. 1 reports the estimated number of endmembers. Two methods for estimating the number of endmembers in the original data set and in the recovered scenes (after coding and decoding) are evaluated: the HySime method [20] and a method developed by Harsanyi, Farrand, and Chang [21] that includes a noise-whitening process as preprocessing to remove the second-order statistical relations (referred to hereinafter as the NWHFC method). It should be noted that, although the number of endmembers was estimated with NWHFC using three different values of false alarm probability ($P_F = 10^{-3}$, $P_F = 10^{-4}$, and $P_F = 10^{-5}$), Fig. 1 only shows the estimation for $P_F = 10^{-4}$. From this figure and ground-truth information

[1] http://aviris.jpl.nasa.gov/html/aviris.freedata.html
[2] http://speclab.cr.usgs.gov/spectral-lib.html

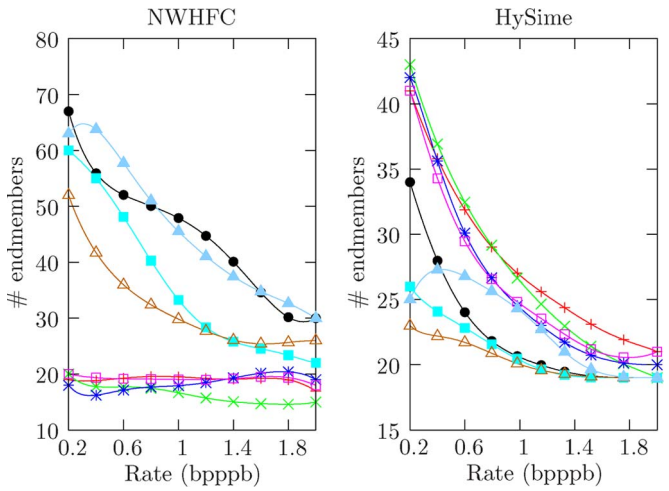

Fig. 1. Estimation of p (the number of endmembers) using the NWHFC method (with $P_F = 10^{-4}$) and the HySime method for the AVIRIS Cuprite scene coded with different compression techniques and compression ratios. The legend is in Fig. 2.

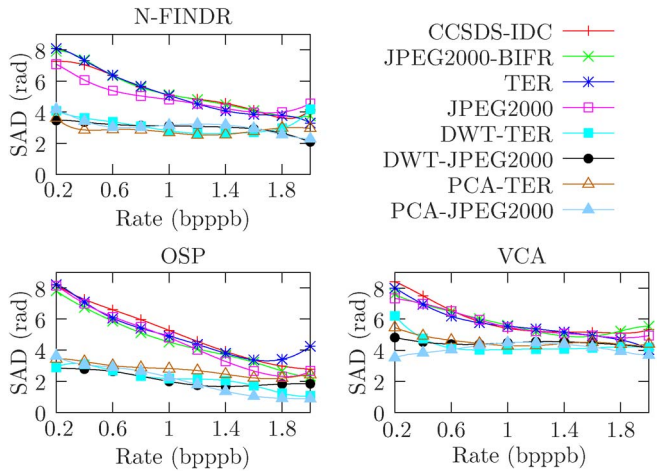

Fig. 2. SAD-based similarity scores, measured in radians, between the endmembers extracted from the original AVIRIS Cuprite data set and the endmembers extracted after coding the original scene with different compression techniques and compression ratios. The values have been multiplied by a constant factor of 100 for visualization purposes.

available online from USGS, a reasonable estimate of the number of endmembers in the original hyperspectral scene seemed to be $p = 22$ (according to estimations by NWHFC using $P_F = 10^{-4}$ or by HySime).

The results reported on Fig. 1 revealed the following aspects. First, the estimation of the number of endmembers in the AVIRIS Cuprite scene by the NWHFC and HySime methods was better for lower compression ratios (high bit rate). As the compression ratio was increased (low bit rate), the use of PCA or DWT for spectral decorrelation severely affected the estimation of the number of endmembers by NWHFC, whereas HySime performed differently, in the sense that the compression techniques applying PCA or DWT performed better than the other ones. For the NWHFC method, we can observe two performance groups: 1) 3-D compression algorithms (DWT-TER, DWT-JPEG2000, PCA-TER, and PCA-JPEG2000) were outperformed by the 2-D compression algorithms (TER, JPEG2000, CCSDS-IDC, and JPEG2000-BIFR). On the other hand, for the HySime method, the most accurate estimates were provided by TER with DWT and PCA as spectral decorrelators, revealing a distinctive behavior than the NWHFC method. These methods are based on different concepts for estimating the number of endmembers, and it is not surprising that their sensitivity to different types and levels of compression is different, as indicated by our experiments.

2) Experiment 2: Impact of Hyperspectral Data Lossy Compression on Endmember Extraction: In the following, we assume that the number of endmembers in the AVIRIS Cuprite scene is $p = 22$ (see Fig. 1). With this assumption in mind, we extracted 22 endmembers from the original and compressed scenes (at different compression ratios) using three popular endmember extraction methods: N-FINDR [22], orthogonal subspace projection (OSP) [23], and vertex component analysis (VCA) [24]. Our quantitative assessment of endmember extraction accuracy was conducted by comparing the results obtained by the same endmember extraction algorithm applied to the original hyperspectral scene (without compression) and to the scenes obtained after applying different compression techniques. The quantitative measure used for evaluation of endmember extraction accuracy was the average spectral angle distance (SAD) between the endmembers obtained from the original scene and the endmembers obtained from the compressed scenes.

Fig. 2 shows the SAD-based similarity scores between the endmembers extracted from the original AVIRIS Cuprite data set and those from the resulting data sets obtained after compressing the original scene with different techniques and compression ratios. The results reported on Fig. 2 indicate that the use of PCA or DWT as spectral decorrelator leads to an improvement in the SAD-based scores for all the endmember extraction algorithms (with lower values meaning higher spectral similarity).

3) Experiment 3: Impact Of Hyperspectral Data Lossy Compression on the Estimation of Abundances: To evaluate the impact of hyperspectral data compression on the process of estimating the abundances of the endmembers extracted from the original and the compressed scenes, we have also conducted an experimental cross validation of the fully constrained linear spectral unmixing (FCLSU) technique described in [25] when combined with the endmembers produced by N-FINDR, OSP, and VCA algorithms. A simple statistical measure to evaluate the similarity of the fractional abundances estimated for the same endmember in the original and the compressed scene is the root MSE (RMSE).

Fig. 3 shows the RMSE-based measures between the abundances estimated for the original scene and those estimated for the compressed scenes, as a function of the compression ratio. The RMSE-based scores of the estimated abundance fractions in this experiment were found to be little dependent, in general, of the compression ratios tested. A possible explanation for this issue is that, although the endmembers extracted from the compressed images may be spectrally degraded due to compression, the spectral signatures of pixels in the scene are also degraded in a similar way. Thus, the FCLSU-based estimation of abundance fractions may lead to RMSE scores, which are overall quite stable, with many of the abundance fractions estimated in the compressed scene being quite similar to those estimated in the original scene.

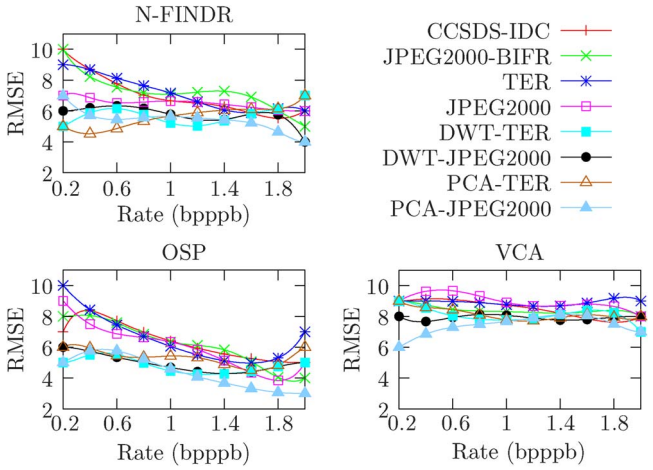

Fig. 3. RMSE-based similarity scores between the abundances estimated from the original AVIRIS Cuprite data set and the abundances estimated after compressing the original scene. The values have been multiplied by a constant factor of 100 for visualization purposes.

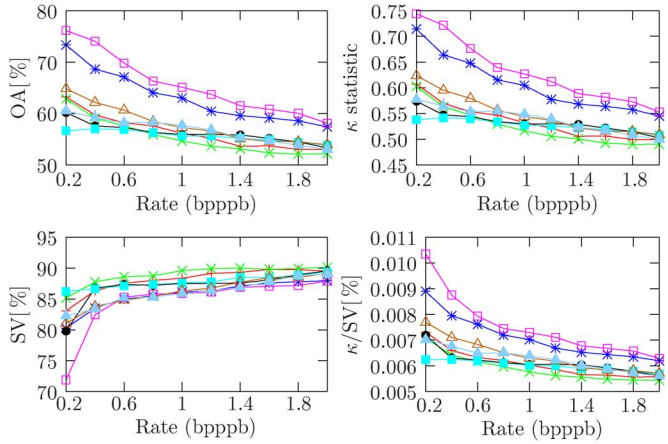

Fig. 4. Classification results obtained with SVM (RBF kernel) on the whole Indian Pines image data set as a function of the compression ratio for different compression techniques. The legend is in Fig. 3.

To conclude this section, we emphasize that the impact of compression on different types of pixels such as *pure* (in which the resulting measure is given by the underlying response of one single material), *mixed* (in which the resulting measure is given by the underlying response of several materials), and *anomalous* (with very low occurrence in the scene) did not reveal important differences when assessing the performance of the compression algorithms.

B. Pixel-Based SVM Classification

The hyperspectral scene used for pixel-based SVM classification experiments is the well-known AVIRIS image (in radiance units) taken over NW Indiana's Indian Pines test site in June 1992. A small portion (145×145) of the original image has been extensively used as a benchmark image for comparing classifiers.[3] In this letter, we consider the whole image, which consists of 614×2166 pixels and 220 spectral bands, with a spatial resolution of 20 m. This data set represents a very challenging land-cover classification scenario. From the 58 different land-cover classes available in the original ground truth, we discarded 20 classes since an insufficient number of training samples were available, and thus, this fact would dismiss the planned experimental analysis. (The background pixels were not considered for classification purposes.) We also removed 20 bands that are noisy or covering the region of water absorption, finally working with 200 spectral bands. Before training, data were normalized to give zero mean and unit variance. Only 20% of the available training samples of each class was used for building the model, and the rest was used for testing.

1) Model Development and Free Parameter Selection: We used an SVM classifier with the radial basis function (RBF) Gaussian kernel because of the good results obtained by this kernel in high-dimensional scenarios and the low percentage of training samples available. Therefore, training the SVM only required tuning the regularization factor C, which was varied in $C = \{10^{-1}, \ldots, 10^{3}\}$, and the kernel Gaussian width σ, which was varied in $\sigma = \{10^{-3}, \ldots, 10^{3}\}$. A nonexhaustive iterative search strategy (τ iterations) was used for tuning these parameters. At each iteration, a sequential search of the estimated kappa statistic (κ) minimum on each parameter domain was performed by splitting the range of the parameter in L points. This minimum was searched using a v-fold strategy on the training set. Values of $\tau = 2$, $L = 10$, and $v = 3$ exhibited the best results in our experiments. A *one-against-one* multiclassification scheme was adopted.

2) Accuracy, Regularization, and Sparsity: Fig. 4 shows several accuracy and complexity measures of the classifiers as a function of the compression ratio for all compression techniques in the test set. We show the overall accuracy, OA[%], the estimated kappa statistic (κ), and the rate of support vectors, SVs[%]. In addition, we also plot the rate κ/SVs[%] that represents a tradeoff between the accuracy and complexity of the classifier. Several conclusions can be drawn from the results reported in Fig. 4.

1) One of the most interesting conclusions that can be obtained is that, for the range of compression ratios used in our experiments, it is possible to get a better performance of the SVM classifier when the compression ratio increases. This is because, after lossy compression, an image is obviously distorted, but this distortion may also result in a local smoothing in the spatial domain, which can, in turn, be advantageous for classification.
2) In all curves, two performance groups are observed: JPEG2000 and TER clearly outperform the rest of the compression techniques. At low compression ratios (high image quality), all the techniques collapse, whereas these two still show better classification performance and yield a controlled complexity in terms of lower rates of support vectors. JPEG2000-BIFR and CCSDS-IDC yield poor performance.
3) We should note that there is a clear tendency to overfit the training data when working with images compressed by JPEG2000-BIFR and CCSDS-IDC. This effect can be explained, because these compression techniques yield higher spatial artifacts and, thus, spatial diversity. In such situations, classifiers need a higher number of support vectors to achieve good performance but, by doing so,

[3] ftp://ftp.ecn.purdue.edu/biehl/MultiSpec/92AV3C.lan

overfitting arises. (Approximately 90% of support vectors and lower accuracy results are observed.) Differences between techniques are clearly observed in all plots, and they are very clear in Fig. 4(d), which contains the proposed criterion of overall model robustness.

As a concluding remark, we must state that regularization is imposed through spatial homogeneity, which is differently managed by different "spatial" preprocessors (image compression techniques): typically, the better the quality of the spatial–spectral smoothing, the higher the classification accuracy.

IV. Conclusions

In this letter, we have quantitatively substantiated the impact of different lossy compression techniques on the tasks of hyperspectral image classification and spectral unmixing. Our experimental results, conducted using two well-known AVIRIS hyperspectral scenes, have revealed some interesting properties that may be useful to image analysts interested in assessing the impact of lossy data compression techniques on the different stages that comprise the pixel-based SVM-based classification and linear spectral unmixing chains.

1) Lossy compression can negatively affect the process of *estimating the number of endmembers*. This is an important limitation since, in most cases, the goal of data compression is to provide users with the compressed data only, and therefore, it would be challenging to accurately estimate the number of endmembers in the original scene using both the current state-of-the-art techniques available in literature (NWHFC and HySime).
2) Even if the quality of the spectral signatures associated to extracted endmembers is degraded by compression, the abundance estimation process can still provide resembling fraction maps if the endmembers are directly extracted from the compressed scene.
3) Better overall classification accuracies and higher sparsity values can be obtained (even for high compression ratios) in pixel-based SVM classification if spatial–spectral smoothing is performed by transform coding techniques.
4) Some compression techniques (such as JPEG2000-BIFR) can lead to oversmoothed classification maps, whereas other techniques (such as JPEG2000) implicitly include spatial regularization in the SVM-based classification stage by means of spatial preprocessing at the compression stage.

Further experimentation with additional hyperspectral scenes and compression techniques may allow extrapolating the observations in this work to different application scenarios. Future research may also include a comparison of classification/unmixing methods with and without feature extraction.

References

[1] R. O. Green, M. L. Eastwood, C. M. Sarture, T. G. Chrien, M. Aronsson, B. J. Chippendale, J. A. Faust, B. E. Pavri, C. J. Chovit, M. Solis, M. R. Olah, and O. Williams, "Imaging spectroscopy and the Airborne Visible/Infrared Imaging Spectrometer (AVIRIS)," *Remote Sens. Environ.*, vol. 65, no. 3, pp. 227–248, Sep. 1998.

[2] G. Motta, F. Rizzo, and J. A. Storer, Eds., *Hyperspectral Data Compression*. Berlin, Germany: Springer-Verlag, 2006.

[3] J. Serra-Sagristà and F. Aulí-Llinàs, "Remote Sensing Data Compression," in *Computational Intelligence for Remote Sensing*. Berlin, Germany: Springer-Verlag, Jun. 2008, pp. 27–61.

[4] B. Penna, T. Tillo, E. Magli, and G. Olmo, "Transform coding techniques for lossy hyperspectral data compression," *IEEE Trans. Geosci. Remote Sens.*, vol. 45, no. 5, pp. 1408–1421, May 2007.

[5] G. Mercier, M.-C. Mouchot, and G. Cazuguel, "Joint classification and compression of hyperspectral images," in *Proc. IEEE IGARSS*, Jul. 1999, vol. 4, pp. 2035–2037.

[6] A. Kaarna, P. Toivanen, and P. Keränen, "Compression and classification methods for hyperspectral images," *Pattern Recognit. Image Anal.*, vol. 16, no. 3, pp. 413–424, Jul. 2006.

[7] M. D. Pal, C. M. Brislawn, and S. P. Brumby, "Feature extraction from hyperspectral images compressed using the JPEG-2000 standard," in *Proc. 5th IEEE SSIAI*, 2002, pp. 168–172.

[8] I. Blanes and J. Serra-Sagristà, "Quality evaluation of progressive lossy-to-lossless remote-sensing image coding," in *Proc. IEEE ICIP*, Nov. 2009, pp. 3665–3668.

[9] T. Kohonen, *Self-Organization and Associative Memory*. New York: Springer-Verlag, 1989.

[10] N. Kasapoglu and O. Ersoy, "Border vector detection and adaptation for classification of multispectral and hyperspectral remote sensing images," *IEEE Trans. Geosci. Remote Sens.*, vol. 45, no. 12, pp. 3880–3893, Dec. 2007.

[11] A. Plaza, P. Martínez, R. Pérez, and J. Plaza, "A quantitative and comparative analysis of endmember extraction algorithms from hyperspectral data," *IEEE Trans. Geosci. Remote Sens.*, vol. 42, no. 3, pp. 650–663, Mar. 2004.

[12] G. Camps-Valls and L. Bruzzone, "Kernel-based methods for hyperspectral image classification," *IEEE Trans. Geosci. Remote Sens.*, vol. 43, no. 6, pp. 1351–1362, Jun. 2005.

[13] Consultative Committee for Space Data Systems (CCSDS), Image Data Compression CCSDS 122.0-B-1, ser. Blue Book, Nov. 2005. [Online]. Available: http://public.ccsds.org/publications/archive/122x0b1.pdf

[14] F. García-Vílchez and J. Serra-Sagristà, "Extending CCSDS recommendation for image compression for remote sensing scenarios," *IEEE Trans. Geosci. Remote Sens.*, vol. 47, no. 10, pp. 3431–3445, Oct. 2009.

[15] D. Taubman and M. Marcellin, *JPEG2000: Image Compression Fundamentals, Standards, and Practice*. Norwell, MA: Kluwer, 2002, ser. International Series in Engineering and Computer Science.

[16] Group on Interactive Coding of Images, TER Software; Open Source CCSDS-122-B-1 Implementation and Extension, Jun. 2009. [Online]. Available: http://www.gici.uab.cat/TER

[17] D. Taubman, Kakadu software, 2000. [Online]. Available: http://www.kakadusoftware.com/

[18] F. Aulí-Llinàs and J. Serra-Sagristà, "JPEG2000 quality scalability without quality layers," *IEEE Trans. Circuits Syst. Video Technol.*, vol. 18, no. 7, pp. 923–936, Jul. 2008.

[19] Group on Interactive Coding of Images, BOI software; Open Source JPEG2000 implementation, Jun. 2009. [Online]. Available: http://www.gici.uab.cat/BOI

[20] J. Bioucas-Dias and J. Nascimento, "Hyperspectral subspace identification," *IEEE Trans. Geosci. Remote Sens.*, vol. 46, no. 8, pp. 2435–2445, Aug. 2008.

[21] C.-I Chang and Q. Du, "Estimation of number of spectrally distinct signal sources in hyperspectral imagery," *IEEE Trans. Geosci. Remote Sens.*, vol. 42, no. 3, pp. 608–619, Mar. 2004.

[22] M. E. Winter, "N-FINDR: An algorithm for fast autonomous spectral end-member determination in hyperspectral data," in *Proc. SPIE Image Spectrometry V*, 2003, vol. 3753, pp. 266–277.

[23] J. C. Harsanyi and C.-I Chang, "Hyperspectral image classification and dimensionality reduction: An orthogonal subspace projection," *IEEE Trans. Geosci. Remote Sens.*, vol. 32, no. 4, pp. 779–785, Jul. 1994.

[24] J. M. P. Nascimento and J. M. Bioucas-Dias, "Vertex component analysis: A fast algorithm to unmix hyperspectral data," *IEEE Trans. Geosci. Remote Sens.*, vol. 43, no. 4, pp. 898–910, Apr. 2005.

[25] D. Heinz and C.-I Chang, "Fully constrained least squares linear mixture analysis for material quantification in hyperspectral imagery," *IEEE Trans. Geosci. Remote Sens.*, vol. 39, no. 3, pp. 529–545, Mar. 2000.